細胞を分譲している．年間に分譲するアンプル数は3,000を超えて年々増加する傾向にあり，2006年度は3,529アンプルであった．また，リソースを海外に分譲する体制も十分に確立しており，年間250アンプル程度を欧米を中心に分譲しているが，近年はアジア諸国への分譲も増加している．

Ⅲ．国際連携

海外ではATCC (American Type Culture Collection) やECACC (European Collection of Animal Cell Cultures) に代表される細胞バンクが点在しており，非常に多くの細胞を保有している．海外のバンクとはJCRB細胞バンク設立当初より緊密に情報交換を行っており，クロスカルチャーコンタミネーションのデータは共通利用できるフォーマットを用いて連携して情報提供を行っている．また，The Society for In Vitro Biologyにおいては細胞バンク委員会が設置され，品質管理方法の標準化や標準株の基準などに関して議論が進められている．その他国際共同研究としてHeLa細胞のクロスコンタミネーション状況に関する調査を実施し報告を行い，経済協力開発機構 (Organization for Economic Co-operation and Development；OECD) においては連携してガイドライン (Human Derived Material Best Practice) を制定するべく活動し，国際連携が積極的に行われている．

Ⅳ．細胞資源の品質に関する調査と研究例

1．マイコプラズマによる細胞の汚染

マイコプラズマは自己増殖能を持つ細菌の1/10程度の大きさの微生物であり，培養細胞と共存して増殖するが，汚染しても培地が濁ったりしないので混入に気付きにくい．汚染した細胞のタンパク質の25%，DNAの25%程度はマイコプラズマ由来のものと考えられ，細胞の増殖や遺伝子発現など多くの細胞機能に影響を与えることが報告されている．2007年に簡易検査法 (Cambrex社製，MycoAlert™) による全国調査を行った結果，900検体中197検体 (約22%) において陽性判定となり，研究室で使われている細胞の汚染が深刻な問題となっていることが明らかとなった．

2．STR (short tandem repeat) 解析によるヒト由来細胞個別識別

STR解析はゲノム中に存在する2～数個の塩基から成る繰り返し配列 [(CAG)n，(GC)n など] の繰り返し回数に個人差があることから，その出現回数を分析することによって個体を識別する方法である．本方法を用いて収集したヒト由来の培養細胞に関する調査を実施してデータを蓄積し，"ヒト培養細胞識別データベース" を構築した．本調査研究においてヒト培養細胞には意外と多くのクロスカルチャーコンタミネーションが発生していると明らかになった．これまでJCRB細胞バンクで収集した，ヒトに由来する培養細胞数は622種であるが，そのうち33種 (約5%) にクロスカルチャーコンタミネーションが見つかったのである．この結果は詳細な実験手法を含めてJCRB細胞バンクのホームページで公開しているのでぜひ参考にしていただきたい (http://cellbank.nibio.go.jp/ のCellIDの欄に公開している)．

3．染色体詳細解析による細胞特性解析

JCRB細胞バンクでは，高度な染色体詳細解析技術 (mFISH法，mBand法，アレイCGH法など) を組み合わせて細胞の特性を解析している．不死化したヒト間葉系幹細胞における染色体詳細解析では，不死化のために導入した遺伝子の種類によっては，長期培養することにより非常に大きな染色体変化をもたらすことが明らかとなり，この結果は再生医療の実現を目指して様々に取り組まれている研究における基礎知見として重要であると考えられる[1]．また，研究に用いた染色体を詳細に解析する技術が，今後再生医療に用いられる種々の細胞の品質評価技術として発展することが期待される．

おわりに

細胞はすでに広く研究に活用される研究資源となっているが，一般の研究者は使用している細胞のマイコプラズマ汚染やクロスコンタミネーションなどの品質管理に手が回らないのが現状である．研究の再現性・信頼性向上のためにも，細胞の質に今一度注目し，細胞バンクに保存されている高品質な細胞を研究に利用されることを希望したい．

文献

1) Takeuchi M, et al: In Vitro Cell Dev Biol Anim (2007) 43: 129-138

小原有弘 (Arihiro Kohara)
独立行政法人 医薬基盤研究所 生物資源研究部 細胞資源研究室 (JCRB細胞バンク)
E-mail：kohara@nibio.go.jp
2002年名古屋市立大学大学院薬学研究科博士課程修了．博士 (薬学)．第一化学薬品株式会社薬物動態研究所，国立医薬品食品衛生研究所変異遺伝部を経て，2005年より現所属，研究員．

水澤 博 (Hiroshi Mizusawa)
独立行政法人 医薬基盤研究所 生物資源研究部 細胞資源研究室 (JCRB細胞バンク)
E-mail：mizusawa@nibio.go.jp

わが国におけるヒト研究資源バンクの現状と今後

——JCRB(Japanese Collection of Research Bioresources)細胞バンク(厚生労働省)から

水澤　博(写真)　小原有弘　増井　徹
(独)医薬基盤研究所生物資源研究部細胞資源研究室

厚生労働省研究資源バンクは，“対がん10ヵ年総合戦略研究”に質の高い培養細胞と遺伝子材料を提供する目的で，国立衛生試験所(現・国立医薬品食品衛生研究所)と国立予防衛生研究所(現・国立感染症研究所)に設置された(1985年)．当時，癌遺伝子の発見に触発され，癌と遺伝子のかかわりに注目が集まり，一気に癌を追い詰めようという機運が高まった時期であった．

研究の推進にあたって，日本の研究体制の脆弱さがたびたび指摘されていたことから，研究材料を分譲する部門を整備して癌研究の推進が試みられたのであった．近年，研究は巨大化してスピードが求められるようになってきており，ひとりの研究者が材料の準備から実験までのすべてにかかわることは困難となり，それぞれの専門機関を育成して分業化をはかる必要があるとわが国でも考えられるようになってきたが，システムの構成力に優れるアメリカでは1950年代から，Coriell Institute for Medical Research(CIMR)やAmerican Type Culture Collection(ATCC)などの細胞分譲機関を整備し，生命科学研究の推進に役立てていた．1980年代に顕在化した経済摩擦は先進諸国に知的資産の囲い込みを促し，多くの国で研究資源バンク設置が進んだ．

わが国で研究資源バンク事業がスタートするとすぐに，培養細胞研究資源は重大な問題を抱えていることが判明した．それはマイコプラズマによる“汚染”と細胞の“誤謬”の問題であったが，研究資源バンクは単に研究材料を収集して提供するだけではなく，収集して提供するまでの間に十分な吟味を加え資源の品質を十分に見極めるところに本質的な意義があることが明らかになってきたのである．1960年代にアメリカで顕在化したヒト培養細胞へのHeLaコンタミの解決にATCCが果たした役割からも明らかであった．著者らは日本で収集した600種のヒト細胞の8%に誤謬があったことを明らかにし，日本人は器用で間違いを犯さないと信じているとしたらそれは迷信であると注意を促している．

その後，ヒトゲノムプロジェクトによりヒト遺伝子の全塩基配列が明らかにされ，細胞の品質管理法に大きな影響を与えたが，培養細胞の誤謬を防止する目的で実施してきた遺伝子検査が細胞提供者のプライバシーを損なうかもしれないというおそれが出てきてしまったのである．現在のところ収集したヒト培養細胞は600種程度なので問題にはならないが，今後，生存中の方々からの試料提供を受ける必要が生じるようになると問題が顕在化すると考えられる．現在でもSNP研究用の健常人1,000名分の対照実験用ゲノムDNA(PSC，JBIC寄託不死化血液細胞とDNA)については，そのおそれを考えて細胞の誤謬を確認するためのデータをとらないことにしている[1]．

さらに問題となりそうな点は，インフォームドコンセントの範囲内で利用するという考え方である．もちろん，患者さんの立場ではインフォームドコンセントで許可した以上の使い方をしてほしくないことは十分理解できるが，一方で研究というのは予想もしなかった点から新しい発見があって，それが人類の知識を増やして疾病の治療を可能にするのである．したがって，予想外の研究に使ってはならないという規制は，研究者にとってたいへんきびしい内容で，今後議論が必要となるのではないだろうか．

現在，提供しているおもなヒト試料は論文などで公知されたものなので，心配している問題は起こらないが，今後，本特集で話題になるような細胞や移植医療に直結するようなヒト試料が多数寄託される時代がくると，こうした問題が顕在化する可能性がある．だからといって問題が指摘されるまで手をこまねいて待っているだけではわれわれに課せられた責任を果たせそうもないので，ヒト試料を扱う際に問題となりそうな倫理的課題についても研究課題と位置づけて検討を進め，ホームページ[2]を通じて問題点を掲載し，掲示板を通じて批判的意見もいただけるようなシステムを整えている．現在，細胞バンクにヒト試料を扱うことに対する批判が直接来ているわけではないが，問題があると考えられる以上，批判をいただけるようなチャンネルを開いておくことは重要であろう．

1) 水澤　博・他：科学，71：1601-1607，2001．
2) http://cellbank.nibio.go.jp/

In Vitro Cell.Dev.Biol.—Animal (2007) 43:129–138
DOI 10.1007/s11626-007-9021-9

Chromosomal instability in human mesenchymal stem cells immortalized with human papilloma virus E6, E7, and hTERT genes

Masao Takeuchi · Kikuko Takeuchi · Arihiro Kohara · Motonobu Satoh · Setsuko Shioda · Yutaka Ozawa · Azusa Ohtani · Keiko Morita · Takashi Hirano · Masanori Terai · Akihiro Umezawa · Hiroshi Mizusawa

Received: 25 January 2007 / Accepted: 27 March 2007 / Published online: 21 May 2007 / Editor: J. Denry Sato

Abstract Human mesenchymal stem cells (hMSCs) are expected to be an enormous potential source for future cell therapy, because of their self-renewing divisions and also because of their multiple-lineage differentiation. The finite lifespan of these cells, however, is a hurdle for clinical application. Recently, several hMSC lines have been established by immortalized human telomerase reverse transcriptase gene (hTERT) alone or with hTERT in combination with human papillomavirus type 16 E6/E7 genes (E6/E7) and human proto-oncogene, Bmi-1, but have not so much been characterized their karyotypic stability in detail during extended lifespan under in vitro conditions. In this report, the cells immortalized with the hTERT gene alone exhibited little change in karyotype, whereas the cells immortalized with E6/E7 plus hTERT genes or Bmi-1, E6 plus hTERT genes were unstable regarding chromosome numbers, which altered markedly during prolonged culture. Interestingly, one unique chromosomal alteration was the preferential loss of chromosome 13 in three cell lines, observed by fluorescence in situ hybridization (FISH) and comparative-genomic hybridization (CGH) analysis. The four cell lines all maintained the ability to differentiate into both osteogenic and adipogenic lineages, and two cell lines underwent neuroblastic differentiation. Thus, our results were able to provide a step forward toward fulfilling the need for a sufficient number of cells for new therapeutic

M. Takeuchi (✉) · K. Takeuchi · A. Kohara · S. Shioda · Y. Ozawa · A. Ohtani · H. Mizusawa
Division of Bioresources,
National Institute of Biomedical Innovation,
Osaka 567-0085, Japan
e-mail: takeuchim@nibio.go.jp

K. Takeuchi
e-mail: takeuchik@nibio.go.jp

A. Kohara
e-mail: kohara@nibio.go.jp

S. Shioda
e-mail: shioda@nibio.go.jp

Y. Ozawa
e-mail: ozaway@nibio.go.jp

A. Ohtani
e-mail: aohtani@nibio.go.jp

H. Mizusawa
e-mail: mizusawa@nibio.go.jp

M. Satoh
Health Science Research Resources Bank,
Osaka 590-0535, Japan
e-mail: satoh@osa.jhsf.or.jp

K. Morita · T. Hirano · A. Umezawa
National Research Institute for Child Health and Development,
Tokyo 157-8535, Japan

K. Morita
e-mail: morita-keiko@aist.go.jp

T. Hirano
e-mail: hirano-takashi@aist.go.jp

A. Umezawa
e-mail: umezawa@1985.jukuin.keio.ac.jp

M. Terai
Department of Reproductive Biology
and Pathology and Innovative Surgery,
National Research Institute for Child Health and Development,
Tokyo 157-8535, Japan
e-mail: terai@nch.go.jp

applications, and substantiate that these cell lines are a useful model for understanding the mechanisms of chromosomal instability and differentiation of hMSCs.

Keywords Human cord blood mesenchymal stem cell · Long-term culture · Karyotype analysis · mFISH CGH · Differentiation

Introduction

Tissue-specific stem cells in various adult tissues are known to be an important source in the regeneration of damaged tissue and maintenance of homeostasis in the tissues in which they reside. Among these stem cells, human mesenchymal stem cell (hMSC) has recently become of great interest in regenerative medicine, not only to replenish their own tissues, but also to give rise to more committed progenitor cells, which can differentiate into other tissues. MSCs in bone marrow have been shown to differentiate into several types of cell such as osteoblasts, adipocytes, chondrocytes, myocytes, and probably also neuronal cells (Okamoto et al. 2002; Takeda et al. 2004; Mori et al. 2005; Saito et al. 2005; Terai et al. 2005). Because of these properties, it is expected that hMSCs are an enormous potential source for future cell therapy. The goal of our study is to establish cell lines with long lifespan and with parental properties for clinical application. However, clinical application using these cells has been met with enormous difficulty, e.g., isolation of a cell population with specific criteria, expansion in vitro system for obtaining a sufficient number of cells without affecting their genomic characteristics and differentiation properties, and their storage in higher viability.

At present, there is a little evidence suggesting whether changes in these properties occur during expansion. Human normal MSCs have a limited capacity to replicate in the 40- to 50-population doubling level (PDL) at the most. To extend their lifespan, we have previously established human mesenchymal cell lines from human umbilical cord blood or bone marrow by immortalization with human telomerase reverse transcriptase (hTERT), human papillomavirus high-risk type 16 E6/E7 genes (HPV16E6/E7) or polycomb gene, Bmi-1 (Takeda et al. 2004; Mori et al. 2005; Terai et al. 2005).

hTERT-immortalization without affecting biological characteristics, despite extensive proliferation, has been reported in bone-marrow-derived hMSCs (Burns et al. 2005), human fibroblast (Milyavsky et al. 2003), and human keratinocyte (Harada et al. 2003), although it has been indicated that there is the possibility that prolonged culture of hTERT-immortalized fibroblasts may favor the appearance of clones carrying potentially malignant alterations (Milyavsky et al. 2003). HPV16, which encodes oncogenes (E6 and E7), can also immortalize hMSCs in vitro. Both E6 and E7 proteins act through their association with tumor suppressor gene products, p53 and retinoblastoma family members (pRb), respectively. E6 accelerates the degradation of the p53 protein, which is essential for cell arrest at the checkpoint in G_1/S and at the mitotic checkpoint when tetraploidy occurs (Cross et al. 1995), as well as at the G_2 phase under damaging conditions. E7 protein binds to pRb and abrogates the repressive function of these cell cycle regulations (Zheng et al. 2001). Thus, both p53 and pRb play a multitude of important roles in cell-cycle-progression checkpoints as reported in human keratinocytes (Patel et al. 2004), and fibroblasts (Khan et al. 1998). As a consequence, the disruption of the checkpoints that govern accurate cell division leads to abnormal segregation of chromosome and genomic instability, as shown in the cells immortalized with HPV16E6/E7 genes (Duensing et al. 2002).

In this paper, we report on the chromosomal instability and the differentiation activity during prolonged culture (cell expansion) using four mesenchymal stem cell lines. These results indicate that an umbilical cord blood-derived clone immortalized with hTERT (UCBTERT-21) showed normal karyotype for a period of 1 yr, whereas three other cell lines immortalized with HPV16E6/E7 and hTERT or HPV16E6, Bmi-1 and hTERT showed chromosomal instability but maintained the ability to differentiate.

Materials and Methods

Cell culture. Human mesenchymal stem cell lines, UCB TERT-21 (JCRB1107), UCB408E6E7TERT-33 (JCRB1110), UE6E7T-3 (JCRB1136), and UBE6T-6 (JCRB1140) were obtained from the JCRB Cell Bank (Osaka, Japan). Two of them are cell lines obtained by immortalizing human umbilical cord blood mesenchymal stem cells (UCB) with hTERT alone (UCBTERT-21; Terai et al. 2005) or with HPV16E6/E7 in combination with hTERT (UCB408E6E7TERT-33; Terai et al. 2005), and the two others are human bone-marrow-derived mesenchymal stem cell lines transformed with HPV16E6/E7 and hTERT genes (UE6E7T-3; Mori et al. 2005) or with bmi-1, HPV16E6 and hTERT genes (UBE6T-6; Takeda et al. 2004; Mori et al. 2005).

The UCBTERT-21 and UCB408E6E7TERT-33 were grown in PLUSOID-M medium (Med-Shirotori Co., Tokyo, Japan) or MSCGM BulletKit (Cambrex Co., East Rutherford, NJ). UE6E7T-3 and UBE6T-6 were cultured in POWEREDBY10 medium (Med-Shirotori Co.) or MSCGM BulletKit (Cambrex Co.); 5×10^3 cells/ml of each cell line were seeded and cultured for 7–10 d. When culture

plate was subconfluent, cells were treated with 0.25% trypsin/0.5 mM EDTA solution (both from Invitrogen, Tokyo, Japan) and replated at a density of 5×10^3 cells/ml.

All of the cells were maintained in a humidified incubator at 37° C and 5% CO_2. PDLs were calculated using the formula: PDL= log (cell output/input)/log2. At the starting cultivation, PDLs of UCBTERT-21, UCB408E6E7 TERT-33, UE6E7T-3, and UBE6T-6 were 42, 67, 60, and 56, respectively. The doubling time of the UCB408E6E7T-33 cell was 1.5 d, and that of UCBTERT-21, UE6E7T-3, or UBE6T-6 was 2.6, 2.0, or 4.0 days, respectively.

Measurement of chromosome number and fluorescence in situ hybridization. Metaphase chromosome spreads for measurement of chromosome number and fluorescence in situ hybridization (FISH) were prepared from exponential growing cells at various PDL. The cells were treated in a hypotonic solution after exposure to 0.06 μg/ml colcemid (Invitrogen, Carlsbad, CA) for 2 h and fixed in methanol/acetic acid (3:1). The cells were spread on a microscope slide.

To count the number of chromosomes, the cells were stained with DAPI (4′-6-diaminido-2-phenylindol; Vector Laboratories, Inc. Burlingame, CA) and examined under an Axioplan II imaging microscope (Carl Zeiss, GmbH) equipped with Leica QFISH software (Leica Microsystems Holding, UK). To examine statistically significant chromosome numbers, we have allowed ±1 deviation and 50–100 metaphase spreads were scored for each assay.

Painting probes specific for chromosome 13 (XCP13-kit, FITC; MetaSystems, GmbH) and chromosome 17 (XCP17-kit; Texas Red) (MetaSystems GmbH, Altlussheim, Germany), and multicolor probes (mFISH-24Xcyte-kit, DAPI, FITC, TexasRed, Cy3, Cy5, and DEAC; MetaSystems GmbH) were used for FISH analysis. FISH was performed according to the manufacture's protocol (MetaSystems GmbH). Briefly, both the metaphase chromosome spread and the probe were denatured with 0.07 N NaOH or 70% formamide, hybridized at 37° C for 1–4 d, and counterstained with DAPI. FISH images were captured and analyzed on the Zeiss Axio Imaging microscope (Carl Zeiss Microimaging GmbH, Jena, Germany) with Isis mBAND/mFISH imaging Software (MetaSystems GmbH).

CGH analysis. Hybridization was carried out with the BAC Array (MAC ArrayTM Karyo 4000 Component, Macrogen Co., Rockville, MD) by the Hybstation (Genomic Solutions, Ann Arbor, MI). Briefly, test DNAs, which were isolated using an isolation kit (Amersham BioSciences, Little Chalfont, UK) and Spin Column (QIAGEN Co., Tokyo, Japan), and reference DNAs (Promega Co., Madison, WI), were labeled, respectively, with Cy3 or Cy5 (BioPrimer DNA Labeling System, Invitrogen Co.), precipitated together with ethanol in the presence of Cot-1 DNA, redissolved in a hybridization mixture (50% formamide, 10% dextran sulfate, 2xSSC, 4% sodium dodecyl sulfate [SDS], pH 7), and denatured at 75° C for 10 min. After incubation at 37° C for 30 min, each mixture was applied to an array slide and incubated at 42° C for 48–72 h. After hybridization, the slides were washed in a solution of 50% formamide—2× SSC (pH 7.0) for 15 min at 50° C, in 2× SSC—0.1% SDS for 15 min at 50° C, and in a 100-mM sodium phosphate buffer containing 0.1% Nonidet P-40 (pH 8) for 15 min at room temperature, then scanned with GenePix4000A (Axon Instruments, Union City, CA). Acquired images were analyzed with MacViewer (Macrogen Instruments).

Differentiation ability. To evaluate the differentiation potential of each cell line, cells were cultured on a coverslip in each induction medium, that is, hMSC Differentiation BulletKit-Adipogenic (PT-3004, Cambrex BioScience, Inc., Walkersville, MD) for adipocyte and NPMM Bullet kit (NPMM™ BulletKit (B3209, Cambrex BioScience) for neural progenitor cells. For osteoblast, cells were treated with 0.1 μM dexamethasone (Sigma Chemical Co., St. Louis, MO), 50 μg/ml L-ascorbic acid (Sigma Chemical), and 10 mM β-glycerophosphate (Sigma Chemical) in the PLUSOID-M medium (Med-Shirotori Co.) or the POWER-EDBY10 medium (Med-Shirotori Co.) of culture medium.

After 2–4 wk, the cells were washed in phosphate-buffered saline (PBS), fixed in 4% paraformaldehyde in PBS and stained with Oil Red-O (Sigma Chemical) for detection of adipocyte, and with alkaline phosphatase staining solution containing 0.25 mg/ml naphthol AS-BI phosphate and 0.25 mg/ml Fast violet LB salt for detection of alkaline phosphatase-positive osteoblast. In immunostaining for neuron-like cells, the cells fixed with paraformaldehyde were permeabilized with methanol at −20° C for 10 min and stained with an anti-IIIβ tubulin antibody (Sigma Chemical) or anti-neurofilament antibody NF-200 (Sigma Chemical) and Texas Red-anti-mouse IgG (Southern Biotechnology Associates, Inc., Birmingham, AL) as previously described (Takeuchi et al. 1990).

Results

Changes in chromosomal number in human mesenchymal stem cell lines in prolonged culture. Immortalization of cultured cells frequently induces an abnormal chromosome number as shown in cancer cells (Duensing et al. 2000; Munger et al. 2004; Patel et al. 2004), especially at higher frequency in long-term culture. We therefore examined four cell lines, human mesenchymal stem cell (hMSC) lines immortalized with combinations of bmi-1, E6, E7, and/or hTERT genes, for chromosome instability by counting metaphase chromosomes.

All of the lines were diploid, each containing 46 up to 40 PDL including the PDL numbers of nontransfecting original MSCs (Takeda et al. 2004; Mori et al. 2005; Terai et al. 2005). For UCBTERT-21 cell, no further changes in chromosome number have been observed up to date (for PDL 133) as shown in Fig. 1*A* and *B*. In contrast, although the UBE6T-6 cell and the UE6E7T-3 cell were near diploid, both cells exhibited considerable variation in chromosome number from PDL 70 after the culture started. For example, when the assay of UE6E7T-3 cells start at PDL 62 in culture, 90% of cell population had 46 chromosomes, but the population decreased with prolonged culturing and a population containing 44 chromosomes became dominant (43% of cell populations) at PDL 147 (Fig. 1*E*, *F*). A similar variation was also observed in UBE6T-6 cells (Fig. 1*C*, *D*).

To ascertain whether or not the changes observed were induced by transfection with HPV16E6E7, we assayed the chromosome numbers of UCB408E6E7TERT-33 cell in prolonged culture. The cell line showed similar chromosomal changes to those of the UE6E7T-3 cell, the rate of which was more rapid. At day 2 after culture by us changes became evident (PDL 68), the UCB408E6E7TERT-33 cells consisted of two distinct populations concerning chromosome number (near diploid [24%] and near tetraploid [53%]), shown in Fig. 1*G*. However, the near diploid population was unstable and decreased gradually. At PDL 81, the population became only near tetraploid, 80% of the

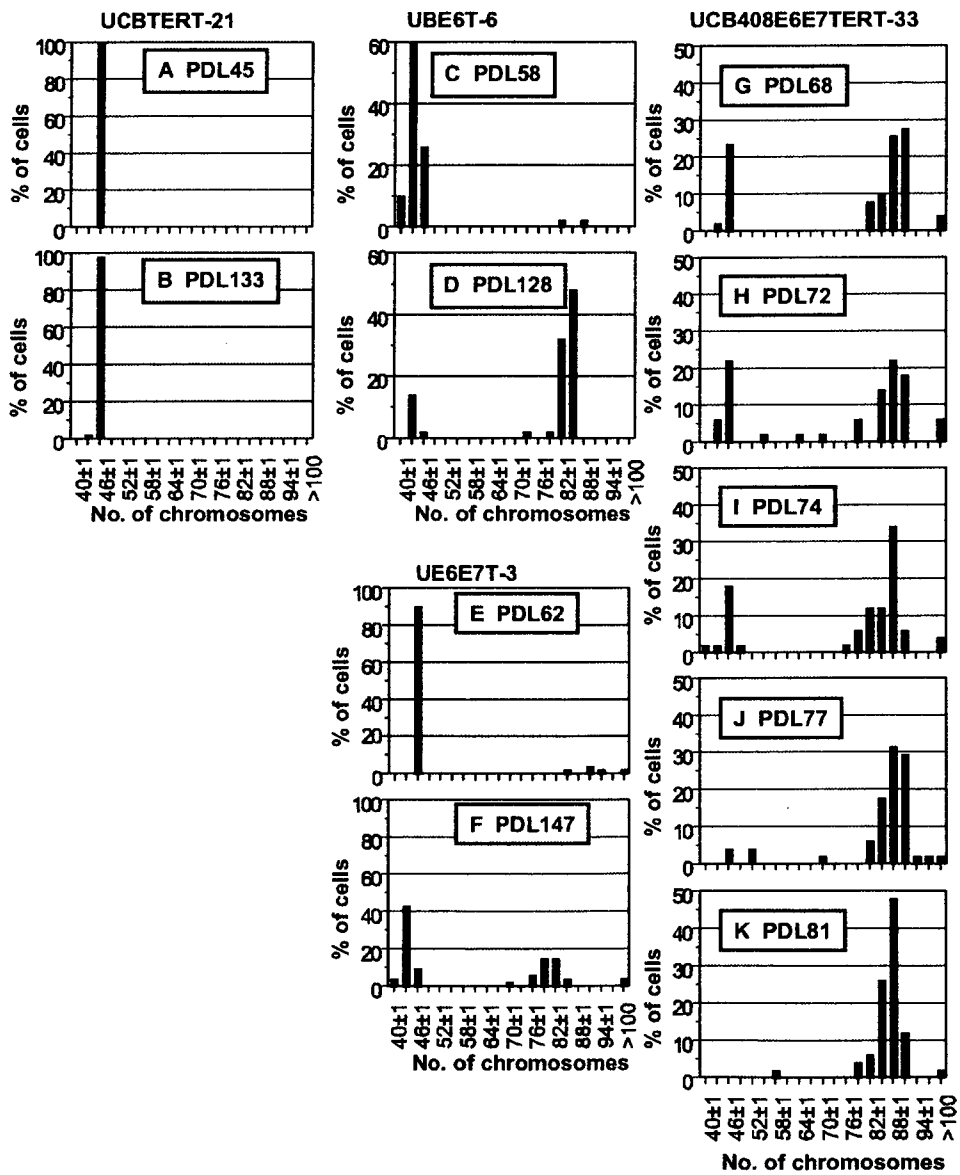

Figure 1. Changes in chromosomal numbers in prolonged cultures of four hMSC cell lines. (*A–K*) The chromosomal numbers at various culture stages were counted by DAPI staining. (*A*, *B*), (*C*, *D*), (*E*, *F*), and (*G–K*) represent the chromosomal numbers from UCBTERT-21, UBE6T-6, UE6E7T-3, and UCB408E6E7TERT-33, respectively. To examine statistically significant chromosomal numbers, we have allowed ±1 deviation, and 50–100 metaphase spreads were examined for each assay. *Note* the changes in chromosomal number from near 2*n* to near 4*n* in prolonged culture.

cells contain 85–92 chromosomes (Fig. 1*K*). The results indicate that UCBTERT-21 is relatively stable in chromosome number, whereas each of the oncogene-immortalized cells (UE6E7T-3, UBE6T-6, and UCB408E6E7TERT-33 cell) were unstable in chromosome numbers, which altered substantially during prolonged culture.

We next applied FISH and CGH analysis to characterize the chromosomal aberrations of the cell lines. All of the four cell lines passed for PDL 50 before examination by FISH. mFISH analysis of the UCBTERT-21 cell at PDL 52 showed normal chromosome composition (Fig. 2*A* and *B*) as observed in non-immortalized cells. The UBE6T-6 cell containing 43–45 chromosomes demonstrates losses of chromosome 13, 16, and 19 (marginal variation in chromosome 4 was observed among cells), but keeps on proliferating in chromosome number of 43–45 (Fig. 2*D*, *E*). In contrast, the UCB408E6E7TERT-33 cell showed more heterogeneity in chromosome composition with intrachromosomal and interchromosomal aberrations (data not shown). However, by mFISH analysis we were able to detect nonrandom losses of chromosome 13 in three cell lines except the UCBTERT-21 cell line. This was also confirmed by pFISH analysis using the probes specific for chromosome 13 and chromosome 17 (Fig. 2*C*, *F*). More than 97% of UCBTERT-21 cells showed two copies for chromosome 13, indicating the stability of the chromosomes in the cell line (Fig. 2*G*). The UE6E7T-3 and the UBE6T-6 cell lines with chromosome numbers of 43–45 showed only one copy of chromosome 13 in 76% of UE6E7T-3 cells and 86% of UBE6T-6 cells, respectively (Fig. 2*I*, *J*). A similar loss of chromosome 13 was also observed in 70% of UCB408E6E7TERT-33 cells, which showed three copies of chromosome 13 in near tetraploid (Fig. 2*H*). Other chromosomes, for example chromosome 17, were contained in the UCBTERT-21 and UBE6T-6 cell lines (Fig. 2*C*, *F*).

Furthermore, a significant nonrandom loss of chromosome 13 at the single cell-level observed by FISH was examined by array CGH, which samples the entire cell population. Figure 3 shows the array CGH profiles from early (*blue spots*) and late (*red spots*) stages of proliferating of each cell line. The UCBTERT-21 cell did not show any detectable differences in array CGH profiles between early and late stages (Fig. 3*A*). Although the loss of chromosome 13 had already occurred at early stages in the UBE6T-6 and the UCB408E6E7TERT-33 cell lines, in addition to the losses of chromosomes 4, 9, and 16 (Fig. 3*B*, *D*), in UE6E7T-3 the loss appeared between PDL 78 to 101 with loss of chromosome 16. The most compelling observation was that all three cell lines revealed a consistent whole loss of chromosome 13. These data are consistent with the results observed by FISH analysis. From these results, we

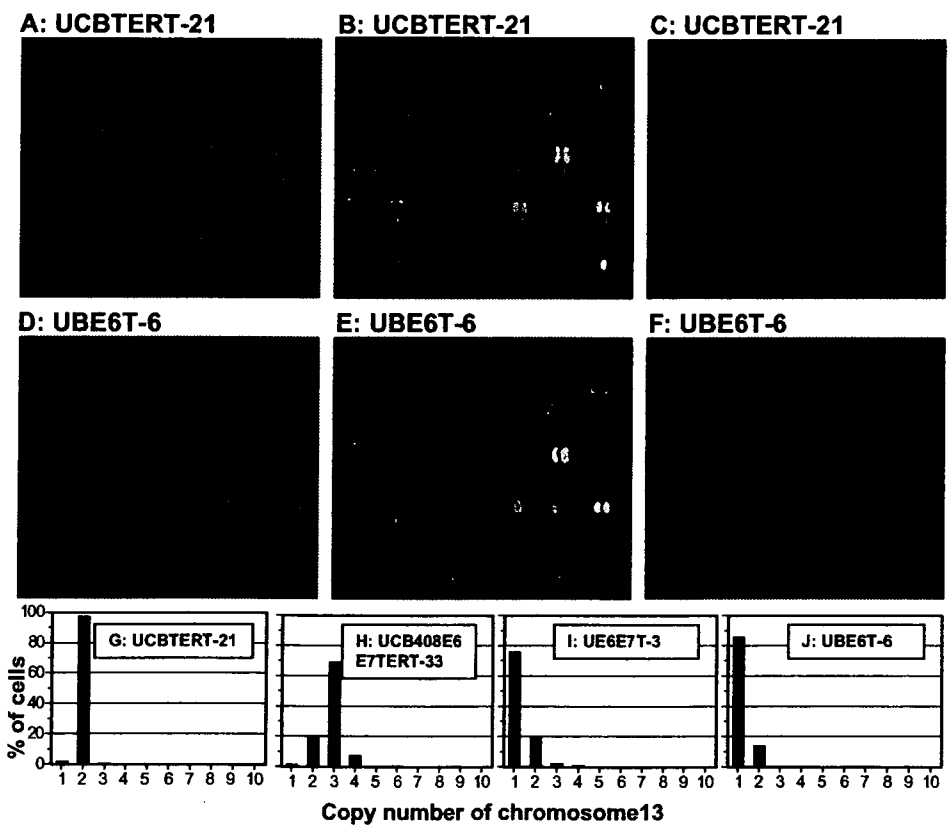

Figure 2. FISH analysis of human mesenchymal stem cell (hMSC) lines immortalized with hTERT alone, hTERT plus bm-1, HPVE6 or with hTERT plus HPVE6/E7. Multicolor FISH images of metaphase spreads (*A*, *D*), their karyotypes (*B*, *E*), and painting FISH images using DNA probes specific for chromosome 13 (*green*) and 17 (*red*) (*C*, *F*) of UCBTERT-21 (*A*, *B*, *C*) and UBE6T-6 (*D*, *E*, *F*). Quantity of chromosome 13 copy numbers in four cell lines (*G*–*J*). FISH signals were counted in 120~200 metaphase spreads plus interphase nuclei. UCBTERT-21 cells contained two copies of chromosome 13 and 17, and showed normal human karyotype, whereas other cells lost one copy of chromosome 13.

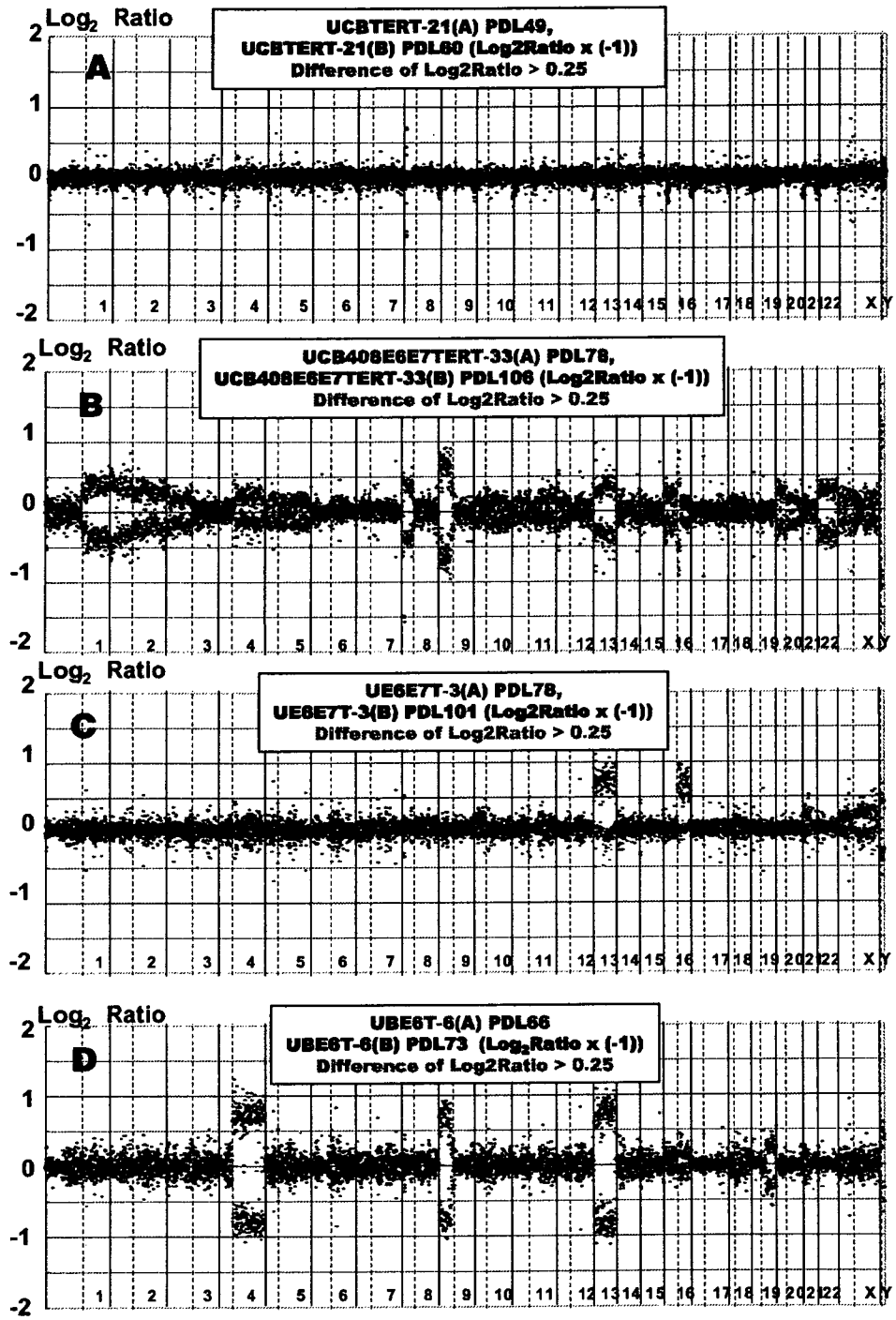

Figure 3. Array CGH profiles performed on four immortalized human mesenchymal stem cell lines at selected PDL. For each *panel*, the *X*-axis represents the 22 autosomes, the *X* and *Y* chromosomes, and the *Y*-axis shows the $\log_2$ of the fluorescence intensity ratio (cy3 [hMSCs]/cy5 [normal cell]) of all spots of the chromosome. Values above 0 (*red spots*) or values below 0 (*blue spots*) signify a loss of chromosome (chromosome regions). *Blue spots* in each *panel* indicate the $\log_2$ ratios observed at early stage in the culture of each cell line, which are overlaid with *red spots* indicated at the late stage. *Green spots* indicate the difference in value between *blue spots* and *red spot*. *Note* that in the UE6E7T-3 cell line, one copy of chromosome 13 and 16 were lost between PDL 78 and 101.

concluded that only hTERT-mediated immortalization induced little change in the chromosome numbers and chromosome structures of mesenchymal stem cells, but immortalization with Bmi-1, E6, and E7 in addition to hTERT results in chromosome instability.

Differentiation potential into lineages of immortalized mesenchymal stem cell lines. It has been reported that mesenchymal stem cells have the extensive potential to differentiate into multiple cell lineages including osteoblast, chondrocytes, adipocytes (Pittenger et al. 1999), cardiac myocytes (Makino et al. 1999), and neural cells (Pacary et al. 2006; Wislet-Gendebien et al. 2005). To evaluate whether chromosome instability of these cell lines in prolonged culture affects differentiation, cells of each cell line were stimulated in each induction medium for 2 to 4 wk. In

adipocyte-specific culture medium, all cell lines accumulated lipid-rich vacuoles in their cytoplasm within 2 wk, which were made evident by Oil Red-O staining. In particular, the UE6E7T-3 cell line showed a greater adipogenetic ability among the four cell lines (Fig. 4*Ab*). In osteoblast induction medium for 2 wk, UCB408E6E7 TERT-33 cells showed a marked increase in alkaline phosphatase expression, a marker of osteoblast, compared with those in the three other cell lines (Fig. 4*Ad*). In addition, UBE6T-6 cells in neuron induction medium reduced proliferation and displayed marked changes in morphology from being a flat-polygonal shape to taking on the characteristic neuron-like shape in which the cells develop long branching processes. Moreover, in comparing the expression patterns of characteristic neural antigens, i.e., neurofilament, III-β-tubulin, before and after induction (28 d), the pseudo-neural shaped cells showed apparent increases in immunoreactivity to both antibodies (Fig. 4*Af, Ah*),

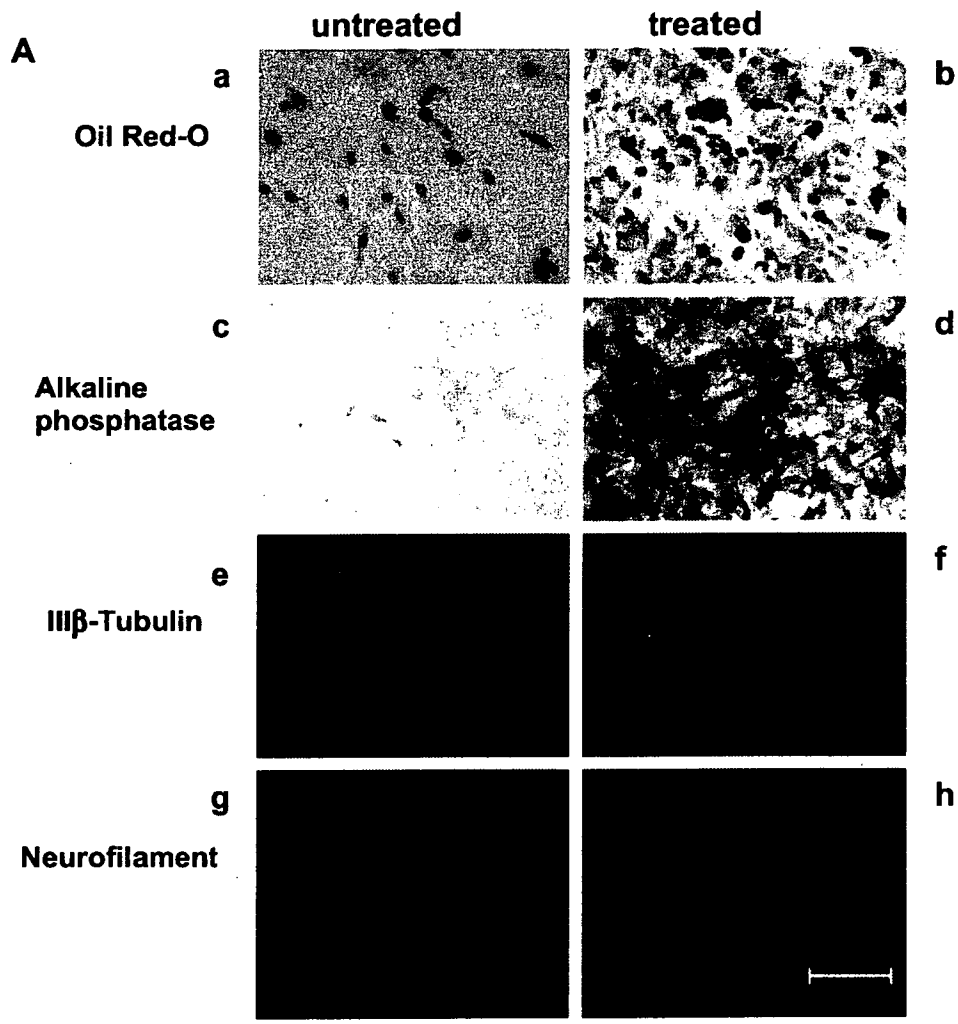

Figure 4. Differentiation potential of immortalized human mesenchymal stem cell lines into adipogenic, osteogenic, and neurogenic lineages. Adipogenesis was indicated by the accumulation of lipid stained with Oil Red-O (*Aa* and *Ab*, UE6E7T-3 cell line). Osteogenesis is indicated by the increase in alkaline phosphatase (*Ac* and *Ad*, UCB408E6E7TERT-33 cell line). Neurogenesis was shown by staining with two kinds of monoclonal antibodies to IIIβ-tubulin and neurofilament, and by shape changes of cell (*Ae–Ah*, UBE6T-6 cell line). *B*, Comparison of the differentiation potential of four cell lines whose responses to stimuli into differentiation were diverse among the cell lines. − and + indicate a response similar to an untreated cell and a weak positive response. +++ indicates a strong response shown by images of treated cells in Fig. 4*A*. (*Bar* indicates 20 μm).

B

	UCBTERT-21	UCB408E6E7TERT-33	UE6E7T-3	UBE6T-6
Oil Red-O	+	++	+++	+
Alkarine phosphatase	+	+++	+	+
IIIβ- Tubulin	-	+	+/-	+++
Neurofilament	-	++	-	++

whereas such changes were not evident with the flat-shaped cells before induction (Fig. 4*Ae*, *Ag*). Additionally, such cells did not undergo such differentiation in culture medium when cultured for as long as 30 d, although faint staining was observed. Figure 4*B* shows the overall results of differentiation potential of the four cell lines into adipogenic, osteogenic, and neurogenic lineages. These immortalized mesenchymal stem cell lines retained the ability to differentiate into three lineages, although among cell lines there are significant variations in response to lineage-specific induction.

Discussion

Attempts to clarify the mechanisms for extending the lifespan of tumor cells have been made for many years, and several genes that have effects on cellular proliferation and survival have become clear (Munger et al. 2002) in addition to the elucidation that the majority of tumor cells express telomerase (hTERT; Armanios et al. 2005). The goal of one of the series of our studies has been to establish cell lines with long lifespan and with parental properties, on the basis of genotypic and phenotypic characterizations, for application to cell-based therapy. We previously established several cell lines (Takeda et al. 2004; Mori et al. 2005; Terai et al. 2005), and the present study demonstrated that UCBTERT-21, the immortalized cell line derived from human umbilical cord blood-derived MSCs with hTERT, has a normal karyotype and has an extended lifespan by at least 133 population doublings, and has the differentiation potential into the adipocyte or osteoblast similar to parental MSCs (Terai et al. 2005), although the potential was weak but clearly positive in this study. The specific environmental cues to initiate the differentiation of hMSCs are not yet clear.

UCBTERT-21 immortalized with hTERT alone can be prolonged without inhibition of the $p16^{INK4A}$/RB pathway (Terai et al. 2005), the result of which is in agreement with reports that hTERT alone significantly extends the lifespan of human fibroblasts, epithelial, and endothelial cells (Bodnar et al. 1998; Chang et al. 2005), without the requirement for molecular alterations in p53/p21 and pRB/$p16^{INK4A}$ pathways (Milyavsky et al. 2003). However, other researchers have indicated that inactivation of the RB/p16 pathway by E7, or downregulation of p16 expression, in addition to increasing telomerase activities, is necessary for expanding the lifespan of human keratinocytes (Dickson et al. 2000; Kiyono et al. 1998). Thus, the possibility that a telomere-independent barrier may operate to prevent immortalization according to cell types has been indicated.

UCB408E6E7TERT-33, UE6E7T-3, and UBE6T-6 are hMSC-clones immortalized with HPV16E6/E7 or polycomb group oncogene Bmi-1, in combination with hTERT. Immortalization of human keratinocyte in vitro using virus-derived oncogenes such as E6 and E7 is based on initial inactivation of the p53 and/or Rb pathways, which are essential for controlling cell cycle progression in response to DNA damage or after induction tetraploidy; therefore, this gene transduction induces chromosomal abnormalities (Solinas-Toldo et al. 1997; Duensing et al. 2002; Patel et al. 2004; Schaeffer et al. 2004). The cell lines used in this study became completely immortal, yet underwent dynamic changes in their chromosome numbers in prolonged culture. Near diploid population in early passage of UCB408E6E7 TERT-33 became near-tetraploid population with prolonged culture without the appearance of intermediate populations (60–70 chromosomes/cell), and thereafter gave rise to a population having smaller numbers of chromosomes than tetraploid. Similar patterns existed, although at a slower rate, in UBE6T-6 cells and UE6E7T-3. These results suggest that HPVE6 and E7 proteins cause tetraploidy that precedes the chromosomal aberration to aneuploid in E6/E7-immotalized hMSCs, as is currently shown in several lines of evidence. For example, in vitro experiments in human cell lines (N/TERT-1 keratinocytes and HeLa cells) demonstrate that chromosome nondisjunction yields tetraploid rather than aneuploid, and that aneuploid may develop through chromosomal loss from tetraploid, although the mechanistic basis for the tetraploid formation still remains to be elucidated (Shi et al. 2005). This is also suggested from evidence that high frequency of tetraproidy is present with aneuploidy in human tumors (Olaharski et al. 2006; Sen 2000). A distinct pattern of aneuploid became apparent using dual-probe FISH and CGH analyses, in which UCB408E6E7TERT-33 cells predominantly exhibited triploid 13 and tetraploidy 17 together with other chromosomal changes as shown in Figs. 2 and 3. However, surprisingly, the loss of one copy of chromosome 13 was also seen in 70–80% of diploid UE6E7T-3 and diploid UBE6T-6 cells retaining two copies of chromosome 17. The loss occurred in PDL 50 in both UE6E7T-6 and UCB408E6E7TERT-33, and between PDL 78 and 101 in UE6E7T-3. Structural and numerical aberrations targeting chromosome 17 are often reported in tumors from various tissues (Olaharski et al. 2006), whereas the pattern that chromosome 13 is lost and chromosome 17 is stable, was common for the three cell lines in this study, indicating the possibility that the loss of chromosome 13 may play an important role in the chromosomal aberration of hMSCs to acquire growth advantages under the given culturing condition. Similar karyotypic changes were evident in cultured human embryonic stem cells, involving the gain of chromosome 17 or chromosome 12 (Carlson et al. 2000; Draper et al. 2004). It is thus conjectured that the aneuploidy developed through chromosomal loss from

diploid cells arises through different mechanisms from tetraploid intermediate.

An alternative explanation for aneuploid formation mechanism independent of tetraploid intermediate is loss of regulation in centrosome duplication, leading to abnormal centrosome amplification and multipolar spindles, resulting in aneuploidy. In addition, centrosome amplification caused by loss of p53 has been shown in cultured mouse cells (Fukasawa et al. 1996), but not in cultured human cells (Kawamura et al. 2004). However, loss of p53 and centrosome amplification has been revealed in human cancer tissue. Our preliminary examination has indicated a weak correlation between centrosome amplification and chromosome number (data not shown). Only 2.4% of UCBTERT-21 cells contained >3 centrosomes per cell, whereas 11.9% of UCB408E6E7TERT-33, 19.1% of UE6E7T-3 and 14.3% of UBE6T-6 cells contained >3 centrosomes per cell. Thus, further study is still needed to clarify the mechanism inducing chromosomal instability in immortalized hMSCs cultured over a long period.

Human mesenchymal stem cells are thought to be multipotent cells that can replicate stem cells and that can differentiate to lineages of mesenchymal tissues including bone, fat, tendon, and muscle. Our results indicated that immortalized hMSCs, except UCBTERT-21, induced changes in chromosome number over prolonged culture, but these cells have still retained the ability to both proliferate and differentiate. Immortalized UBE6T-6 cells also displayed neuron-like morphology and strong expression of the neuron-specific markers of neurofilament and III-β-tubulin. We previously demonstrated that hTERT, E7-immortalized hMSCs differentiate into neural cells in vitro on the basis of morphological changes, expression of neural markers such as nestin, neurofilament, MAP-2, Nurr1, and III-β-tubulin. Furthermore, the physiological function showed reversible calcium uptake in response to extracellular potassium concentration (Mori et al. 2005). Similar observations have been reported using rat MSCs (Wislet-Gendebien et al. 2003; Wislet-Gendebien et al. 2005; Pacary et al. 2006). In preliminary experiment of cell transplantation that 10^6 cells of UCBTERT-21 cell (PDLs 120) or UCB408E6E7TERT-33 cell (PDLs 200) were injected into nude mice subcutaneously, no tumorigenicity was observed (data not shown).

In conclusion, our study showed that the hTERT-immortalized cell line displayed normal karyotype and differentiation ability in prolonged culture. These results provide a step forward toward supplying a sufficient number of cells for new therapeutic approaches. In addition, oncogene-immortalized cell lines exhibited abnormal karyotype accompanying the preferential loss of chromosome 13 but without differential alteration during prolonged culture. Thus, the results could provide a useful model for understanding the mechanisms of the chromosomal instability and the differentiation of hMSC.

Acknowledgments This study was supported in part by a grant from the Ministry of Health, Labor and Welfare of Japan. We are grateful to Dr. T.Masui for his advice on ethics problems, and to Mr. H.Migitaka (Carl Zeiss Co., Ltd.) for his assistance with mFISH karyotype analysis. M.T. and K.T. contributed equally to this work.

References

Armanios, M.; Greider, C. W. Telomerase and cancer stem cells. Cold Spring Harbor Symp. Quant. Biol. 70:205–208; 2005.

Bodnar, A. G.; Ouellette, M.; Frolkis, M.; Holt, S. E.; Chiu, C. P.; Morin, G. B.; Harley, C. B.; Shay, J. W.; Lichtsteiner, S.; Wright, W. E. Extension of life-span by introduction of telomerase into normal human cells. Science 279:349–352; 1998.

Burns, J. S.; Abdallah, B. M.; Guldberg, P.; Rygaard, J.; Schroder, H. D.; Kassem, M. Tumorigenic heterogeneity in cancer stem cells evolved from long-term cultures of telomerase-immortalized human mesenchymal stem cells. Cancer Res. 65:3126–3135; 2005.

Carlson, J. A.; Healy, K.; Tran, T. A.; Malfetano, J.; Wilson, V. L.; Rohwedder, A.; Ross, J. S. Chromosome 17 aneusomy detected by fluorescence in situ hybridization in vulvar squamous cell carcinomas and synchronous vulvar skin. Am. J. Pathol. 157:973–983; 2000.

Chang, M. W.; Grillari, J.; Mayrhofer, C.; Fortschegger, K.; Allmaier, G.; Marzban, G.; Katinger, H.; Voglauer, R. Comparison of early passage, senescent and hTERT immortalized endothelial cells. Exp. Cell Res. 309:121–136; 2005.

Cross, S. M.; Sanchez, C. A.; Morgan, C. A.; Schimke, M. K.; Ramel, S.; Idzerda, R. L.; Raskind, W. H.; Reid, B. J. A p53-dependent mouse spindle checkpoint. Science 267:1353–1356; 1995.

Dickson, M. A.; Hahn, W. C.; Ino, Y.; Ronfard, V.; Wu, J. Y.; Weinberg, R. A.; Louis, D. N.; Li, F. P.; Rheinwald, J. G. Human keratinocytes that express hTERT and also bypass a p16(INK4a)-enforced mechanism that limits life span become immortal yet retain normal growth and differentiation characteristics. Mol. Cell Biol. 20:1436–1447; 2000.

Draper, J. S.; Smith, K.; Gokhale, P.; Moore, H. D.; Maltby, E.; Johnson, J.; Meisner, L.; Zwaka, T. P.; Thomson, J. A.; Andrews, P. W. Recurrent gain of chromosomes 17q and 12 in cultured human embryonic stem cells. Nat. Biotechnol. 22:53–54; 2004.

Duensing, S.; Lee, L. Y.; Duensing, A.; Basile, J.; Piboonniyom, S.; Gonzalez, S.; Crum, C. P.; Munger, K. The human papillomavirus type 16 E6 and E7 oncoproteins cooperate to induce mitotic defects and genomic instability by uncoupling centrosome duplication from the cell division cycle. Proc. Natl. Acad.Sci. U. S. A. 97:10002–10007; 2000.

Duensing, S.; Munger, K. The human papillomavirus type 16 E6 and E7 oncoproteins independently induce numerical and structural chromosome instability. Cancer Res. 62:7075–7082; 2002.

Fukasawa, K.; Choi, T.; Kuriyama, R.; Rulong, S.; Vande Woude, G. F. Abnormal centrosome amplification in the absence of p53. Science 271:1744–1747; 1996.

Harada, H.; Nakagawa, H.; Oyama, K.; Takaoka, M.; Andl, C. D.; Jacobmeier, B.; von, W. A.; Enders, G. H.; Opitz, O. G.; Rustgi, A. K. Telomerase induces immortalization of human esophageal keratinocytes without p16INK4a inactivation. Mol. Cancer Res. 1:729–738; 2003.

Kawamura, K.; Izumi, H.; Ma, Z.; Ikeda, R.; Moriyama, M.; Tanaka, T.; Nojima, T.; Levin, L. S.; Fujikawa-Yamamoto, K.; Suzuki, K.; Fukasawa, K. Induction of centrosome amplification and

chromosome instability in human bladder cancer cells by p53 mutation and cyclin E overexpression. Cancer Res. 64:4800–4809; 2004.

Khan, S. H.; Wahl, G. M. p53 and pRb prevent rereplication in response to microtubule inhibitors by mediating a reversible G1 arrest. Cancer Res. 58:396–401; 1998.

Kiyono, T.; Foster, S. A.; Koop, J. I.; McDougall, J. K.; Galloway, D. A.; Klingelhutz, A. J. Both Rb/p16INK4a inactivation and telomerase activity are required to immortalize human epithelial cells. Nature 396:84–88; 1998.

Makino, S.; Fukuda, K.; Miyoshi, S.; Konishi, F.; Kodama, H.; Pan, J.; Sano, M.; Takahashi, T.; Hori, S.; Abe, H.; Hata, J.; Umezawa, A.; Ogawa, S. Cardiomyocytes can be generated from marrow stromal cells in vitro. J. Clin. Invest. 103:697–705; 1999.

Milyavsky, M.; Shats, I.; Erez, N.; Tang, X.; Senderovich, S.; Meerson, A.; Tabach, Y.; Goldfinger, N.; Ginsberg, D.; Harris, C. C.; Rotter, V. Prolonged culture of telomerase-immortalized human fibroblasts leads to a premalignant phenotype. Cancer Res. 63:7147–7157; 2003.

Mori, T.; Kiyono, T.; Imabayashi, H.; Takeda, Y.; Tsuchiya, K.; Miyoshi, S.; Makino, H.; Matsumoto, K.; Saito, H.; Ogawa, S.; Sakamoto, M.; Hata, J.; Umezawa, A. Combination of hTERT and bmi-1, E6, or E7 induces prolongation of the life span of bone marrow stromal cells from an elderly donor without affecting their neurogenic potential. Mol. Cell Biol. 25:5183–5195; 2005.

Munger, K.; Baldwin, A.; Edwards, K. M.; Hayakawa, H.; Nguyen, C. L.; Owens, M.; Grace, M.; Huh, K. Mechanisms of human papillomavirus-induced oncogenesis. J. Virol. 78:11451–11460; 2004.

Munger, K.; Howley, P. M. Human papillomavirus immortalization and transformation functions. Virus Res. 89:213–228; 2002.

Okamoto, T.; Aoyama, T.; Nakayama, T.; Nakamata, T.; Hosaka, T.; Nishijo, K.; Nakamura, T.; Kiyono, T.; Toguchida, J. Clonal heterogeneity in differentiation potential of immortalized human mesenchymal stem cells3, Biochem. Biophys. Res. Commun. 295:354–361; 2002.

Olaharski, A. J.; Sotelo, R.; Solorza-Luna, G.; Gonsebatt, M. E.; Guzman, P.; Mohar, A.; Eastmond, D. A. Tetraploidy and chromosomal instability are early events during cervical carcinogenesis. Carcinogenesis 27:337–343; 2006.

Pacary, E.; Legros, H.; Valable, S.; Duchatelle, P.; Lecocq, M.; Petit, E.; Nicole, O.; Bernaudin, M. Synergistic effects of CoCl(2) and ROCK inhibition on mesenchymal stem cell differentiation into neuron-like cells. J. Cell Sci. 119:2667–2678; 2006.

Patel, D.; Incassati, A.; Wang, N.; McCance, D. J. Human papillomavirus type 16 E6 and E7 cause polyploidy in human keratinocytes and up-regulation of G2-M-phase proteins. Cancer Res. 64:1299–1306; 2004.

Pittenger, M. F.; Mackay, A. M.; Beck, S. C.; Jaiswal, R. K.; Douglas, R.; Mosca, J. D.; Moorman, M. A.; Simonetti, D. W.; Craig, S.; Marshak, D. R. Multilineage potential of adult human mesenchymal stem cells. Science 284:143–147; 1999.

Saito, M.; Handa, K.; Kiyono, T.; Hattori, S.; Yokoi, T.; Tsubakimoto, T.; Harada, H.; Noguchi, T.; Toyoda, M.; Sato, S.; Teranaka, T. Immortalization of cementoblast progenitor cells with Bmi-1 and TERT. J. Bone Miner. Res. 20:50–57; 2005.

Schaeffer, A. J.; Nguyen, M.; Liem, A.; Lee, D.; Montagna, C.; Lambert, P. F.; Ried, T.; Difilippantonio, M. J. E6 and E7 oncoproteins induce distinct patterns of chromosomal aneuploidy in skin tumors from transgenic mice. Cancer Res. 64:538–546; 2004.

Sen, S. Aneuploidy and cancer. Curr. Opin. Oncol. 12:82–88; 2000.

Shi, Q.; King, R. W. Chromosome nondisjunction yields tetraploid rather than aneuploid cells in human cell lines. Nature 437:1038–1042; 2005.

Solinas-Toldo, S.; Durst, M.; Lichter, P. Specific chromosomal imbalances in human papillomavirus-transfected cells during progression toward immortality. Proc. Natl. Acad. Sci. U. S. A 94:3854–3859; 1997.

Takeda, Y.; Mori, T.; Imabayashi, H.; Kiyono, T.; Gojo, S.; Miyoshi, S.; Hida, N.; Ita, M.; Segawa, K.; Ogawa, S.; Sakamoto, M.; Nakamura, S.; Umezawa, A. Can the life span of human marrow stromal cells be prolonged by bmi-1, E6, E7, and/or telomerase without affecting cardiomyogenic differentiation? J. Gene Med. 6:833–845; 2004.

Takeuchi, K.; Kuroda, K.; Ishigami, M.; Nakamura, T. Actin cytoskeleton of resting bovine platelets. Exp. Cell Res. 186:374–380; 1990.

Terai, M.; Uyama, T.; Sugiki, T.; Li, X. K.; Umezawa, A.; Kiyono, T. Immortalization of human fetal cells: the life span of umbilical cord blood-derived cells can be prolonged without manipulating p16INK4a/RB braking pathway. Mol. Biol. Cell 16:1491–1499; 2005.

Wislet-Gendebien, S.; Hans, G.; Leprince, P.; Rigo, J. M.; Moonen, G.; Rogister, B. Plasticity of cultured mesenchymal stem cells: switch from nestin-positive to excitable neuron-like phenotype. Stem Cells 23:392–402; 2005.

Wislet-Gendebien, S.; Leprince, P.; Moonen, G.; Rogister, B. Regulation of neural markers nestin and GFAP expression by cultivated bone marrow stromal cells. J. Cell Sci. 116:3295–3302; 2003.

Zheng, L.; Lee, W. H. The retinoblastoma gene: a prototypic and multifunctional tumor suppressor. Exp. Cell Res. 264:2–18; 2001.

In Vitro Cell.Dev.Biol.—Animal (2007) 43:168–175
DOI 10.1007/s11626-007-9033-5

Species identification of animal cells by nested PCR targeted to mitochondrial DNA

Kazumi Ono · Motonobu Satoh · Touho Yoshida · Yutaka Ozawa · Arihiro Kohara · Masao Takeuchi · Hiroshi Mizusawa · Hidekazu Sawada

Received: 5 March 2007 / Accepted: 17 April 2007 / Published online: 22 May 2007 / Editor: J. Denry Sato

Abstract We developed a highly sensitive and convenient method of nested polymerase chain reaction (PCR) targeted to mitochondrial deoxyribonucleic acid (DNA) to identify animal species quickly in cultured cells. Fourteen vertebrate species, including human, cynomolgus monkey, African green monkey, mouse, rat, Syrian hamster, Chinese hamster, guinea pig, rabbit, dog, cat, cow, pig, and chicken, could be distinguished from each other by nested PCR. The first PCR amplifies mitochondrial DNA fragments with a universal primer pair complementary to the conserved regions of 14 species, and the second PCR amplifies the DNA fragments with species-specific primer pairs from the first products. The species-specific primer pairs were designed to easily distinguish 14 species from each other under standard agarose gel electrophoresis. We further developed the multiplex PCR using a mixture of seven species-specific primer pairs for two groups of animals. One was comprised of human, mouse, rat, cat, pig, cow, and rabbit, and the other was comprised of African green monkey, cynomolgus monkey, Syrian hamster, Chinese hamster, guinea pig, dog, and chicken. The sensitivity of the PCR assay was at least 100 pg DNA/reaction, which was sufficient for the detection of each species of DNA. Furthermore, the nested PCR method was able to identify the species in the interspecies mixture of DNA. Thus, the method developed in this study will provide a useful tool for the authentication of animal species.

Keywords Cell line authentication · Cross-contamination · Quality control · Bio-resources

K. Ono · M. Satoh (✉) · T. Yoshida · H. Sawada
Health Science Research Resources Bank (HSRRB),
Japan Health Sciences Foundation,
2-11-Rinku-minamihama, Semnan-shi,
Osaka 590-0535, Japan
e-mail: hsrrb@osa.jhsf.or.jp

Y. Ozawa · A. Kohara · M. Takeuchi · H. Mizusawa
Japanese Collection of Research Bioresources (JCRB),
Division of Bioresources,
National Institute of Biomedical Innovation,
7-6-8 Saito-Asagi, Ibaraki-shi,
Osaka 567-0085, Japan

Introduction

It has been occasionally reported that cell lines derived from a certain source can be contaminated with another cell line. This cross-culture contamination is a serious problem for investigations using culture cells (Nelson-Rees et al. 1981). Therefore, it is very important to confirm the identities of cell lines as part of quality control in the operation of the cell banks that supply these cells to researchers. Some methods have been developed for the authentication of cell lines. For example, short tandem repeat profiling has been used to identify human-origin cell lines (Tanabe et al. 1999; Masters et al. 2001). As for the methods to detect interspecies cross-contamination, chromosome typing, immunological testing, and isoenzyme analysis have been used (Montes de Oca et al. 1969; Stulberg 1973; Doyle et al. 1990). Each of these methods, however, has disadvantages, such as chromosome analysis, which requires great skill, and immunological identification, which requires species-specific antibodies. Isoenzyme analysis is a general method to find

interspecies cross-contamination (Steube et al. 1995). However, the sensitivity of this technique is not suitable for the detection of intermingling with other species-derived cells (Nims et al. 1998), and some specialized reagents and devices are required.

The identification of species by polymerase chain reaction (PCR) based on species-specific deoxyribonucleic acid (DNA) sequences has many advantages, as follows: (1) the equipment required for PCR has become widespread in the laboratories of life science research, (2) the method is relatively simple and does not require great skill, and (3) the sensitivity is high because of amplification of a specific DNA fragment. Thus, some PCR methods for identification of animal species, including cell line authentication, have been reported in recent years (Naito et al. 1992; Hershfield et al. 1994; Parodi et al. 2002; Liu et al. 2003; Steube et al. 2003). However, these methods are not suitable for the purpose of rapidly distinguishing many kinds of animal species.

In the present study, we developed a highly sensitive PCR method that can distinguish 14 animal species, which are commonly used in cell cultures for life science research: i.e., human, cynomolgus monkey, African green monkey, mouse, rat, Syrian hamster, Chinese hamster, guinea pig, rabbit, dog, cat, cow, pig, and chicken.

Materials and Methods

Cell lines and preparation of DNA. All cell lines used in this study are shown in Table 1 and are available from the Health Science Research Resources Bank (HSRRB). These cell lines were confirmed to be free of microorganisms, such as mycoplasma, bacteria, fungi and yeast, and the species in the original description was authenticated by isoenzyme analysis at the HSRRB. Cellular DNA containing both nuclear and mitochondrial DNA was extracted using MagExtractor-Genome (Toyobo. Co., Ltd., Osaka, Japan) according to the manufacturer's instruction, and the resultant purified DNA was used for PCR.

Primer design. The information of full-length and partial mitochondrial DNA sequences for 14 species of animals were obtained from the published database at the National Center for Biotechnology Information (NCBI). The accession numbers of the reference sequences and the area corresponding to each primer's target are listed in Table 2, and the nucleotide sequences of each primer are presented in Table 3. The first primers, which were complementary to conserved sequences within cytochrome *b* (for forward primer) and 16S ribosomal RNA genes (for reverse) among the 14 species, were designed as a universal primer pair (Fig. 1). The amplified product covers cytochrome *b*, d-loop, 12S ribosomal RNA and 16S ribosomal RNA genes, and the predicted product size is 4–5 kbp. The species-specific sequences within the area amplified by the universal primer pair were selected as second primer pairs. To clearly identify the species-specific bands in agarose gel electrophoresis, we designed 2nd primers for the 14 species to amplify different sizes of DNA in the range of 200–1400 bp at approximately 50-bp intervals (Table 2; see also Fig. 3*A*).

Polymerase chain reaction. The 50-µl reaction mixture contained 1.25 units Takara Ex Taq (Takara Bio, Inc., Otsu, Japan), Ex Taq buffer (Mg^{2+}: 2 mM), dNTPs (50 µM each), 10 pmol of each primer and 100 ng of sample DNA, unless otherwise stated. The amplification was carried out in a PCR Thermal Cycler MP (TP3000; Takara Bio Inc.). In the first PCR, the reaction mixture was heated at 94° C for 5 min, at 59° C for 5 min, followed by 35 cycles of elongation at 72° C for 2.5 min, denaturation at 94° C for 30 s, annealing at 59° C for 45 s, with elongation at 72° C

Table 1. Cell lines used in this study

Name of cell line	Registry number	Species
293	JCRB9068	Human
A549	JCRB0076	Human
COLO320 DM	JCRB0225	Human
HuH-7	JCRB0403	Human
HeLa S3	JCRB9010	Human
Hep G2	JCRB1054	Human
JTC-12	JCRB0607	Cynomolgus monkey
MK.P3	JCRB0607.1	Cynomolgus monkey
COS-7	JCRB9127	African green monkey
Vero	JCRB9013	African green monkey
3T3-L1	JCRB9014	Mouse
A9	JCRB0221	Mouse
B16 melanoma	JCRB0202	Mouse
KUM3	JCRB1134	Mouse
WEHI-3b	IFO50296	Mouse
C6	IFO50110	Rat
L6	JCRB9081	Rat
Py-3Y1-S2	JCRB0736	Rat
WB-F344	JCRB0193	Rat
BHK(C-13)	JCRB9020	Syrian hamster
RPMI 1846	JCRB9087	Syrian hamster
CHO-K1	IFO50414	Chinese hamster
TG-1	JCRB0626	Chinese hamster
104C1	JCRB9036	Guinea pig
SIRC	IFO50020	Rabbit
MDCK	IFO50071	Dog
CRFK	JCRB9035	Cat
PG4(S+L−)	JCRB9125	Cat
MDBK	JCRB9028	Cow
PK(15)	JCRB9030	Pig
DT40	JCRB9130	Chicken
LMH	JCRB0237	Chicken
4G12 hybridoma	IFO50090	Hybrid (human × mouse)
N18-RE-105	IFO50221	Hybrid (mouse × rat)

Table 2. The target sequence position for each primer pair in the mitochondrial genome and the predicted size of the amplified product

Species	Primer						Reference mitochondrial DNA sequence (NCBI accession number)
	First primer		Second primer				
	Forward	Reverse	Forward	Reverse	Genes amplified	Predicted product size (bp)	
Human	15226–15249	2990–3009	15311–15334	15732–15751	Cyt b	441	NC 001807
Cynomolgus monkey	479–502[a]	1572–1591[b]	209–229[c]	1320–1340[c]	12S→16S	1132	(a)AF295584, (b)AF420036, (c)AF424970
African green monkey	14643–14666	2408–2427	800–823	1074–1100	12S→16S	301	AY863426.1
Mouse	14623–14646	2430–2449	28–55	954–975	tRNA-Phe→12S	948	NC 005089
Rat	14602–14625	2419–2438	1748–1767	2218–2240	16S	493	NC 001665
Syrian hamster	479–502	ND[a]	682–703	906–926	Cyt b	245	AF119265
Chinese hamster	14604–14627	2413–2432	353–376	930–953	12S	601	DQ390542
Guinea pig	14642–14665	2494–2413	140–159	454–478	12S	339	NC 000884
Rabbit	14653–14676	2425–2444	116–136	799–819	12S	704	NC 001913
Dog	14668–14691	2428–2447	1105–1125	1838–1859	16S	755	AY729880
Cat	15516–15539	3288–3307	1675–1694	3046–3065	12S→16S	1391	NC 001700
Cow	14991–15014	2781–2800	401–421	1469–1490	tRNA-Phe→16S	1090	AB074965
Pig	15791–15814	3568–3587	2099–2123	2898–2917	12S→16S	819	AY337045
Chicken	15383–15406	3715–3734	3395–3415	3570–3591	16S	197	AB086102

Cyt b cytochrome b, *tRNA-Phe* phenylalanine transfer RNA, *12S* 12S ribosomal RNA, and *16S* 16S ribosomal RNA

[a] The corresponding 16S ribosomal RNA genome sequence of Syrian hamster was not available.

[a] means reference sequence AF295584.

[b] means reference sequence AF420036.

[c] means reference sequence AF424970.

for 10 min in the last cycle, and stored at 4° C. The first amplified product was diluted to 1:10 with sterile distilled water, and a 1 μl aliquot of the diluted product was used as the sample DNA for the second PCR. In the second PCR, the reaction mixture was heated to 94° C for 5 min, maintained at 60° C for 5 min, followed by 30 cycles of elongation at 72° C for 1.5 min, denaturation at 94° C for 45 s, annealing at 60° C for 30 s, with elongation at 72° C for 10 min in the last cycle, and stored at 4° C. Each 5 μl of second PCR product was run on a 2% agarose (SeaKem GTG agarose; Cambrex Bio Science Rockland, Inc., Rockland, ME) minigel unless otherwise noted, stained

Table 3. Nucleotide sequences of each primer pair

Primer pair	Forward sequence	Reverse sequence
First PCR primer	THGTHSAATGAATCTGAGGVGGVT	CGATGTTGGATCAGGACATC
Second PCR primer		
Human	TATTGCAGCCCTAGCAGCACTCCA	AGAATGAGGAGGTCTGCGGC
Cynomolgus monkey	AGTGAGCGCAAACGCCACTGC	GTTAACAGTGAAGGTGGCATG
African green monkey	CCAGAAGACCCACGATAACTCTCA	TGTTAGCTCAAGGTAATCGAGTTGTAC
Mouse	GCACTGAAAATGCTTAGATGGATAATTG	CCTCTCATAAACGGATGTCTAG
Rat	CAATCCACCAAGCACAAGTG	CCCCAACCGAAATTTGGTAGTTC
Syrian hamster	GACCTCTTAGGTGTATTCCTAC	GTATGAAGAAGGGGTAGAGCA
Chinese hamster	CCGGCGTAAAACGTGTTATAGACT	GTATTAGGTATAATATCGGCAGTC
Guinea pig	GCCCTATGTACCACACTCAG	CCTTAGCTTTCGTGTGTCGGACTTA
Rabbit	CATGCAAGACTCCTCACGCCA	GGGCTTTCGTATATTCTGAAG
Dog	GCCCAACTAACCCCAAACTTA	GGTTAACAATGGGGTGGATAAG
Cat	TAGAACACCCACGAAGATCC	CATATGGTCTCTTTGGGTCG
Cow	CCTAGATGAGTCTCCCAACTC	GTTGTTTAGTCGAGAGGGTATC
Pig	CCTATATTCAATTACACAACCATGC	GCGTGTGCGAGGAGAAAGGC
Chicken	GTATTCCCGTGCAAAAACGAG	CTTAGTGAAGAGTTGTGGTCTG

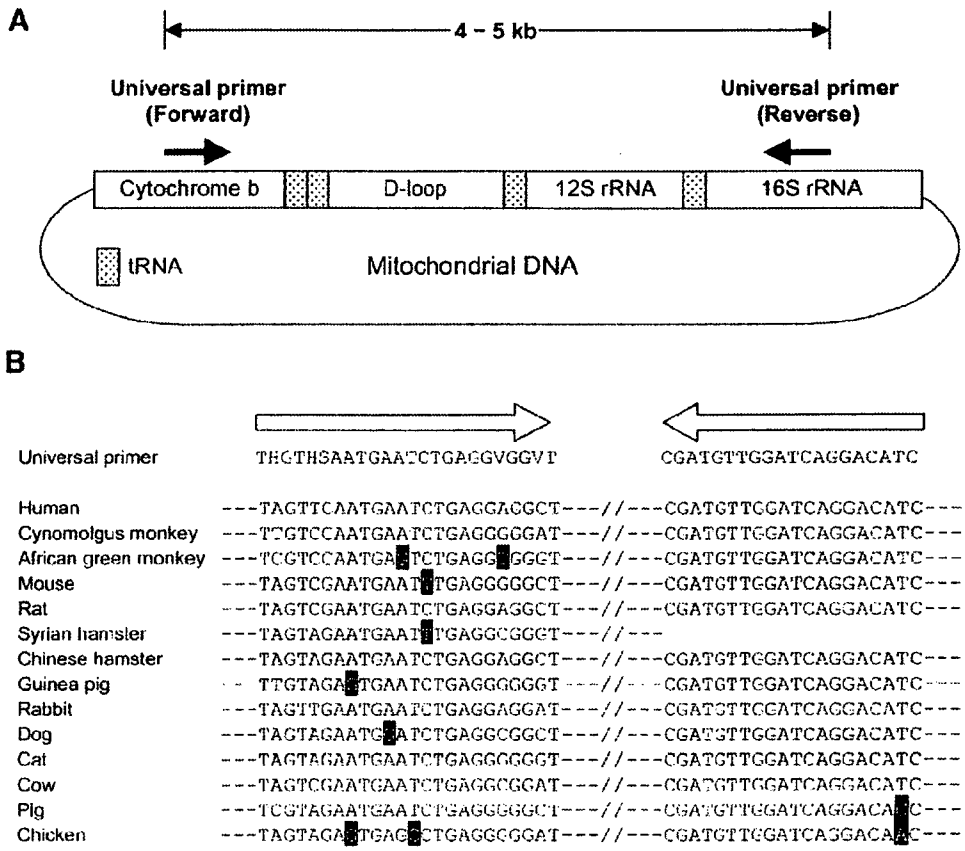

Figure 1. Universal primer pairs for the first PCR. (*A*) The target position in the mitochondrial DNA. The first PCR is expected to amplify 4- to 5-kb DNA fragments spanning from cytochrome *b* to 16S rRNA. (*B*) The sequences of the universal primers and the target nucleotide of 14 animal species. The forward primer was designed to be complementary to the conserved sequences within cytochrome *b* and the reverse primer within 16S ribosomal RNA, respectively. Degenerate primer was used for the forward primer, i.e., H:A/C/T, S:C/G, V:A/C/G. Inversed letters indicate bases mismatched to universal primer sequences. The 16S rRNA sequence of Syrian hamster for reverse primer was not available from the NCBI database.

with ethidium bromide, visualized under UV light (Mupid-Scope WD; Advance Co., Ltd., Tokyo, Japan), and photographed. The 100 bp DNA Ladder (Takara Bio Inc.) was applied as a size marker.

Result and Discussion

First PCR. Mitochondrial DNA is generally a desirable target for PCR compared with nuclear DNA, as each animal cell generally contains 500–1,000 copies of mitochondrial DNA. Primers were designed as described in "Materials and Methods". Figure 2 shows the gel electrophoresis of the first PCR products amplified with the universal primer pair from each species DNA. The predicted 4- to 5-kbp products were clearly observed for all species, except for chicken. In the case of chicken, no visible band was observed at ca. 5 kbp, the size predicted from chicken mitochondrial DNA sequence. However, it is likely that specific amplification does occur during the first PCR for chicken DNA, because a much larger amount of chicken DNA was required without first PCR for identification during the second PCR compared with that obtained when first PCR was carried out (data not shown).

Species-specificity of nested PCR. The nested PCR strategy was used to specifically amplify species-specific DNA. To confirm amplification by each species-specific primer pair, DNA prepared from each cell line originating from 14 species of animals was subjected to the nested PCR using the universal primer pair in the first PCR and the respective single species-specific primer pair in the second PCR. The amplified product from the corresponding species DNA exhibited the predicted size (Table 2) for each animal species, and could be readily distinguished from each other according to the different sizes (Fig. 3*A*). Figure 3*B* shows the species-specificity of nested PCR in this strategy. Most of the species-specific primer pairs, i.e., human, cynomolgus monkey, Syrian hamster, Chinese ham-

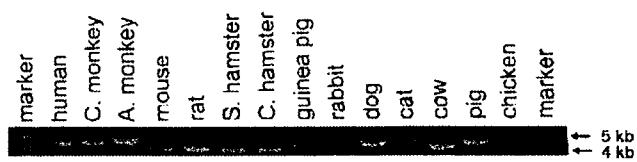

Figure 2. Gel electrophoresis of first-PCR products for 14 species. DNA of each species was extracted from the following cell lines indicated in *parentheses*, human (A549), cynomolgus monkey (MK.P3), African green monkey (COS-7), mouse (*WEHI-3b*), rat (Py-3Y1-S2), Syrian hamster (BHK-1 (C-13)), Chinese hamster (CHO-K1), guinea pig (104C1), rabbit (SIRC), dog (MDCK), cat (PG-4(S+L−)), cow (MDBK), pig (PK15), chicken (LMH) for amplification using the universal primer pair. The amplified DNA fragments were run on a 1% agarose gel.

ster, guinea pig, dog, cat, cow, pig, and chicken primers, amplified the specific DNA only from the corresponding species DNA. In the PCR using primer pairs specific for rabbit and African green monkey, however, unexpected bands appeared in addition to the predicted ones. The rabbit primer pair amplified cynomolgus monkey DNA, but the product could be readily distinguished from the rabbit-specific band because of their different sizes. The primer pair for African green monkey also produced an approximately 300-bp-sized band for cynomolgus monkey DNA, which was similar in size

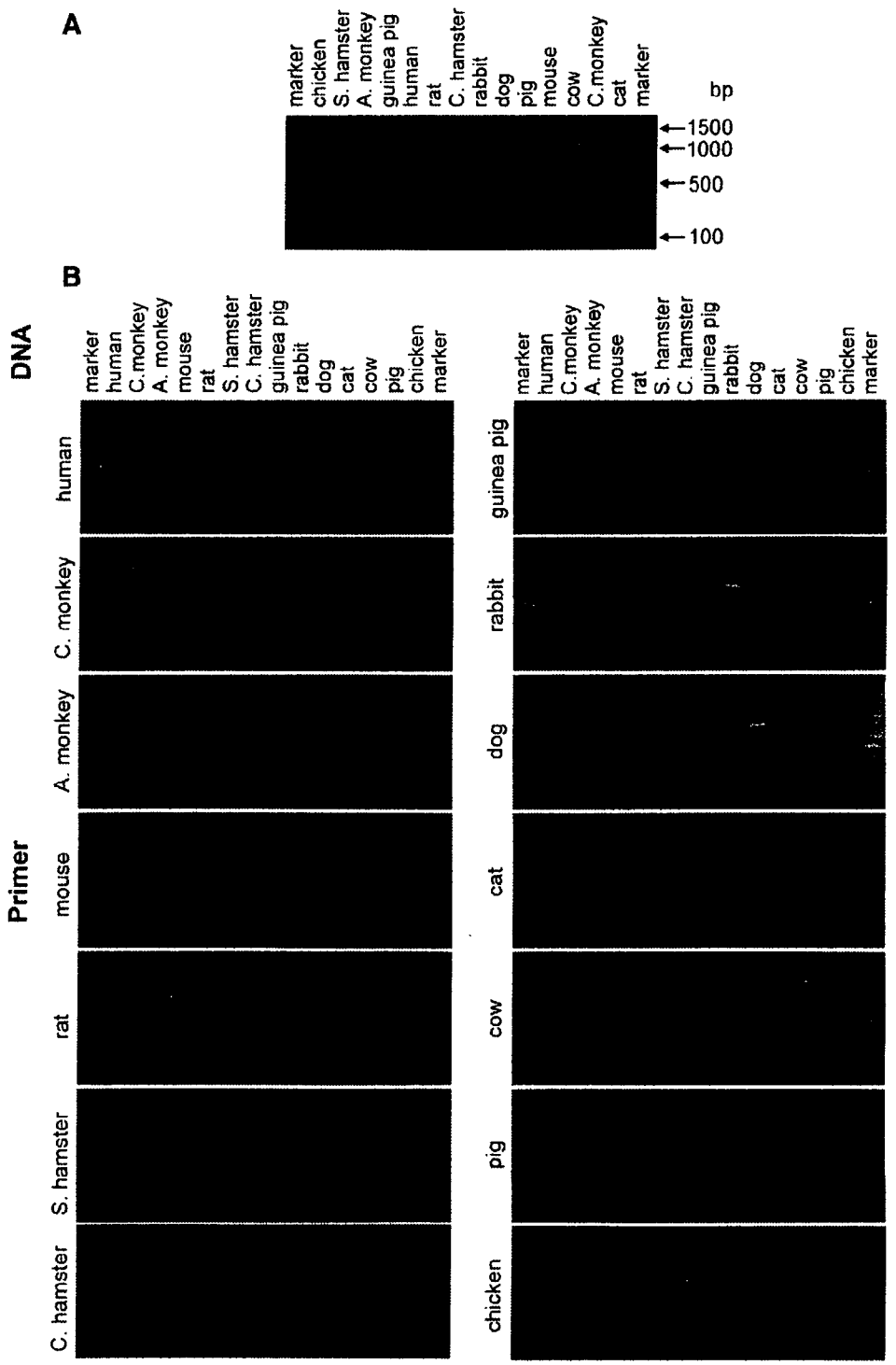

Figure 3. Gel electrophoresis of the second-PCR products for 14 species. The same cell lines as in Fig. 2 were used. (*A*) DNA of each species was subjected to nested PCR using corresponding species-specific primer pairs in the second PCR. The second-PCR products were aligned in size-order as a ladder. The amplification products were distinguished by the size. (*B*) Species specificity of the nested PCR. The 14 species-derived DNA was amplified with the universal primer pair and further amplified with the second primer pair indicated on the left side of each photograph.

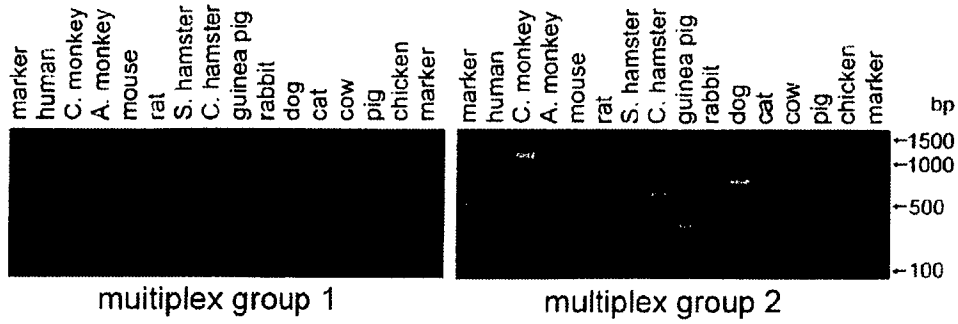

Figure 4. Gel electrophoresis of multiplex-PCR products. The first amplification products for 14 species DNA were subjected to multiplex PCR using the mixture of seven species-specific primer pairs as follows. Multiplex group 1: the primer mixture for human, mouse, rat, rabbit, cat, cow, and pig. Multiplex group 2: the primer mixture for cynomolgus monkey, African green monkey, Syrian hamster, Chinese hamster, guinea pig, dog, and chicken. The cell lines used for each animal are the same as described in Fig. 2.

to the African green monkey-specific product. This may be caused by some degree of sequence similarity between African green monkey and cynomolgus monkey in the target mitochondrial DNA. Indeed, when the mixture of primer pairs for African green monkey and cynomolgus monkey were applied to the second PCR, the nonspecific amplified product from cynomolgus monkey DNA disappeared, possibly because of competition of primer annealing to the target DNA sequences (data not shown; *see* also the result in the multiplex PCR section). Thus, it was confirmed that the nested PCR strategy is very useful for the identification of 14 species of DNA.

Multiplex PCR assay: For the simple and rapid identification of 14 species of animals, multiplex PCR was examined using primer mixtures in the second PCR. As a result of testing many combinations, it was favorable that the 14 kinds of species-specific primer pairs were divided into two groups as follows: Group 1 contained primer pairs for human, mouse, rat, rabbit, cat, cow, and pig, and Group 2 contained primers for cynomolgus monkey, African green monkey, Syrian hamster, Chinese hamster, guinea pig, dog, and chicken. Figure 4 shows the result of multiplex PCR. These animal species, divided into the two groups, could be clearly detected as species-specific bands. Most of the amplification products were specific for each primer mixture, but nonspecific bands were slightly observed for cynomolgus monkey and African green monkey when multiplex group 1 was used. These nonspecific bands were readily distinguished from the specific ones according to their sizes. Thus, it was found that multiplex PCR assay is applicable to simultaneous identification of 14 species of animals by dividing into two groups. The method developed here is superior to the previous PCR methods (Naito et al. 1992; Hershfield et al. 1994; Parodi et al. 2002; Liu et al. 2003; Steube et al. 2003) in identifying many kinds of species generally used for life science studies. In particular, this method has a great advantage in distinguishing Chinese hamster from Syrian hamster, as the cell lines such as CHO and BHK derived from these two kinds of hamsters are very popular for cell cultures.

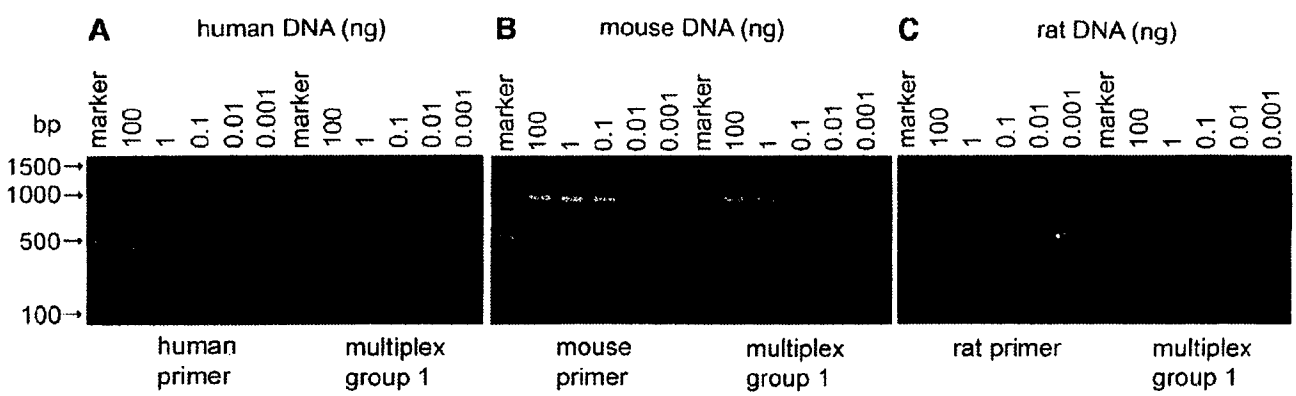

Figure 5. Gel electrophoresis of nested-PCR products for serially diluted DNA. The sample DNA was extracted from the human A549 cell line (*A*), mouse WEHI-3b cell line (*B*), and rat Py-3Y1-S2 cell line (*C*), and diluted serially to the nested PCR. The product bands amplified by single species-specific primer pairs are shown on the *left side* and those by multiplex group 1 are on the *right* in each photograph.

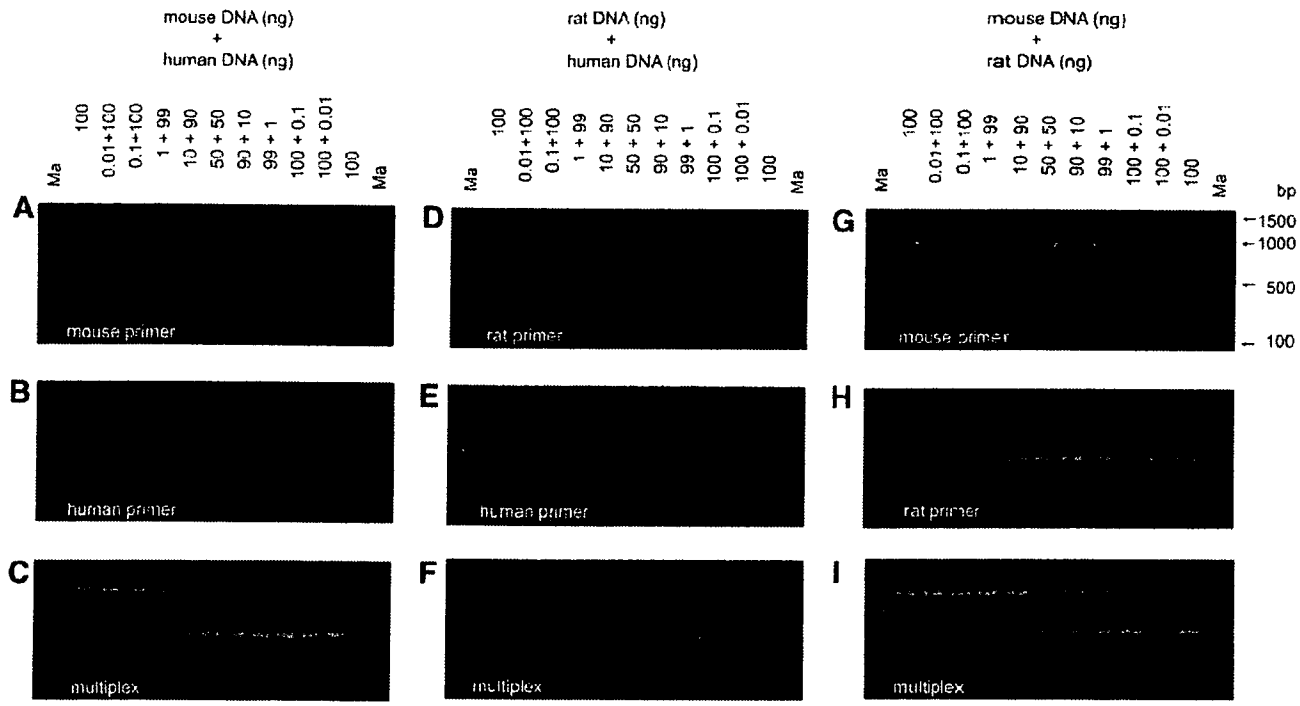

Figure 6. Gel electrophoresis of nested-PCR products for interspecies DNA mixtures. Two kinds of DNA, such as human and mouse DNA (*A*, *B*, *C*), human and rat DNA (*D*, *E*, *F*), and mouse and rat DNA (*G*, *H*, *I*) were mixed in various ratios for amplification with nested PCR. The cell lines used were the same as in Fig. 5. In the second PCR, the single species-specific primer pairs (*A*, *B*, *D*, *E*, *G*, *H*) or the multiplex group 1 (*C*, *F*, *I*) were used.

Sensitivity of PCR assay. Serially diluted cellular DNA was amplified with the nested PCR using either the corresponding species-specific primer pair or the mixture of seven species-specific primer pairs (multiplex PCR described above) as the second PCR primer. Each of the 14 species of DNA was detectable from at least 100 pg DNA/reaction by both PCR assays. Figure 5 shows the sensitivity of the PCR assay, as an example, using DNA prepared from human, mouse, and rat cell lines, which are commonly used for cell culture experiments. The amount of DNA required for identification of each species was 10 pg/reaction or more for the single species-specific primer pair as the second primer, and 100 pg/reaction or more for the multiplex assay. The sensitivity of the multiplex assay was somewhat low compared to the species-specific single primer.

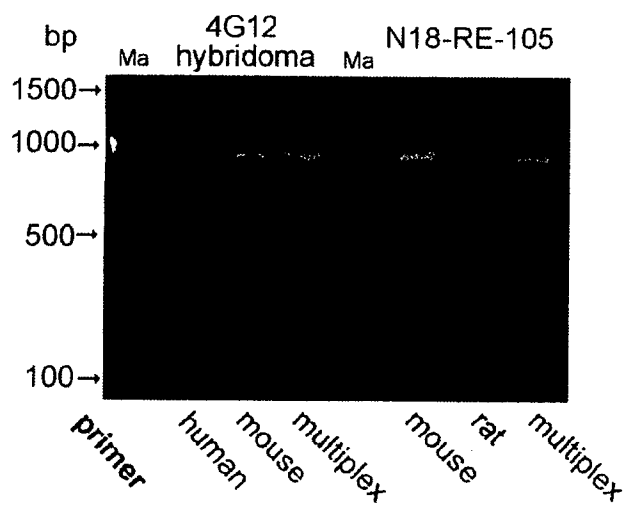

Figure 7. Gel electrophoresis of nested-PCR products for DNA derived from interspecies hybrid cell lines. DNA from 4G12 hybridoma (human + mouse) and N18-RE-105 (mouse + rat) were applied to nested PCR. Multiplex group 1 or the corresponding species-specific primer pairs were used in the second PCR.

Identification of species from interspecies DNA mixtures. The possibility of cross-contamination or replacement of cells exists during the process of cell preparation. As part of the quality control of cell lines in the cell bank, it is very important to verify the source species of each derived cell line. For that purpose, we attempted to identify the species from interspecies DNA mixtures. Two species of DNA, among human, mouse and rat, were mixed in various ratios for the nested PCR. When the single species-specific primer pair was used in the second PCR, each species of DNA was sensitively detected even when two kinds of DNA were present in the mixture. For example, when mouse-specific primers were used, a mouse-specific band was detected in the DNA mixture composed of 100 ng human or rat DNA + 10 pg mouse DNA (Fig. 6*A*, *G*). Likewise, in the case of human-specific or rat-specific primers alone, their respective species-specific band was also detected at 10 pg DNA

(Fig. 6*B, E, D, H*). When group 1 of the multiplex primers (seven species-specific primer pairs composed of human, mouse, rat, rabbit, cat, cow, and pig) was used at the standard concentration (10 pmol each species-specific primer/50-μl reaction), the sensitivity apparently decreased and there was considerable difference in the sensitivity for human, mouse, and rat DNA (Fig. 6*C, F, I*). This may be caused by the different amplification efficiency of each species-specific primer in the simultaneous reaction. Indeed, by decreasing the ratio of human primer pairs relative to the others, the sensitivity for mouse and rat DNA clearly increased (data not shown). Thus, this method will likely become a very useful tool for quickly detecting cross-contamination, and the sensitivity in the multiplex assay will be further increased by optimizing the concentration and the ratio of species-specific primers.

Hybrid cell lines. We applied this PCR method to original-species verification of interspecies hybrid cell lines. The hybrid cell lines of 4G12 (human B lymphocytes × mouse myeloma cell line; Saito et al. 1988) and N18-RE-105 (mouse glioma cell line × rat neural retina cells; Malouf et al. 1984) were tested by isoenzyme analysis and nested PCR. Although the original species were confirmed by isoenzyme analysis of both hybridomas between human and mouse, and between mouse and rat, only the mouse-specific band was observed for both hybridomas by nested PCR (Fig. 7). This result is consistent with the previous reports that the mouse mitochondria dominate selectively in these hybrid cells, whereas human or rat mitochondria are ultimately excluded from the hybrid cells (Attardi and Attardi 1972; Yamaoka et al. 2001). The nested PCR method targeted to the mitochondria genome was not applicable to the parental species identification of interspecies hybrid cells.

References

Attardi, B., Attardi, G. Fate of mitochondrial DNA in human-mouse somatic cell hybrids. Proc Nat Acad Sci USA. 129–133; 1972.

Doyle, A., Morris, C., Mowles, J. M. Quality control. In: Doyle, A, Hay, R., Kirsop, B. E. eds. Living resources for biotechnology. Animal cells. Chapter 5. Cambridge: Cambridge University Press; 1990: 81–100.

Hershfield, B., Chader, G., Aguirre, G. A polymerase chain reaction-based method for the identification of DNA samples from common vertebrate species. Electrophoresis. 15: 880–884; 1994.

Liu, M. Y., Lin, S., Liu H., Candal, F., Vafai A. Identification and authentication of animal cell culture by polymerase chain reaction amplification and DNA sequencing. In Vitro Cell Dev Biol Anim. 39: 424–427; 2003.

Malouf, A. T., Schnaar, R. L., Coyle, J. T. Characterization of a glutamic acid neurotransmitter binding site on neuroblastoma hybrid cells. J Biol Chem. 259: 12756–12762; 1984.

Masters, J. R., Thomson, J. A., Daly-Burns, B., Reid, Y. A., Dirks, W. G., Packer, P., Toji, L. H., Ohno, T., Tanabe, H., Arlett, C. F., Kelland, L. R., Harrison, M., Virmani, A., Ward, T. H., Ayres, K. L., Debenham, P. G. Short tandem repeat profiling provides an international reference standard for human cell lines. Proc Nat Acad Sci USA. 98: 8012–8017; 2001.

Montes de Oca, F., Macy, M. L., Shannon, J. E. Isoenzyme characterization of animal cell culture. Proc Soc Exp Biol Med. 132: 462–469; 1969.

Naito, E., Dewa, K., Yamanouchi, H., Kominami, R. Ribosomal ribonucleic acid (rRNA) gene typing for species identification. J Forensic Sci. 37: 396–403; 1992.

Nelson-Rees, W. A., Daniels, D. W., Flandermeyer, R. R. Cross-contamination of cells in culture. Science. 212: 446–452; 1981.

Nims, R. W. Shoemaker, A. P., Bauemschub, M. A., Rec L. J., Harbell, J. W. Sensitivity of isoenzyme analysis for the detection of interspecies cell line cross-contamination. In Vitro Cell Dev Biol Anim. 34: 35–39; 1998.

Parodi, B., Aresu, O., Bini, D., Lorenzini, R., Schena, F., Visconti, P., Cesaro, M., Ferrera, D., Andreotti, V., Ruzzon, T. Species identification and confirmation of human and animal cell lines: a PCR-based method. BioTechniques. 32: 432–440; 2002.

Saito, H., Uchiyuma, K., Nakamura, I., Hiraoka, H., Yamaguchi, Y., Taniguchi, M. Characterization of a human monoclonal antibody with broad reactivity to malignant tumor cells. J Natl Cancer Inst. 80. 728–734; 1988.

Steube, K. G., Grunicke, D., Drexler, H. G. Isoenzyme analysis as a rapid method for the examination of the species identity of cell cultures. In Vitro Cell Dev Biol Anim. 31. 115–119; 1995.

Steube, K. G., Meyer, C., Uphoff, C. C., Drexler, H. G. A simple method using β-globin polymerase chain reaction for the species identification of animal cell lines—a progress report. In Vitro Cell Dev Biol Anim. 39: 468–475; 2003.

Stulberg, C. S. Extrinsic cell contamination of tissue culture. In: Fogh, J. ed. Contamination in tissue culture. New York: Academic Press; 1973:2–23.

Tanabe, H., Takada, Y., Mitegishi, D., Kurematsu, M., Masui, T., Mizusawa, H. Cell line individualization by STR multiplex system in the cell bank found cross-contamination between ECV304 and EJ-1/T24. Tissue Culture Research Communications. 18: 329–338; 1999.

Yamaoka, M., Mikami, T., Ono, T., Nakada, K., Hayashi, J. Mice with only rat mtDNA are required as models of mitochondrial diseases. Biochem Biophys Res Commun. 282: 707 711; 2001.